International Conferences on Recent Advances in Geotechnical Earthquake Engineering and Soil Dynamics

2001 - Fourth International Conference on Recent Advances in Geotechnical Earthquake Engineering and Soil Dynamics

30 Mar 2001, 10:30 am - 12:30 pm

Analytical Study of the Nikawa Landslide

Dimitrious Loukidis
Purdue University, West Lafayette, IN

Sang-Ho Lee
Purdue University, West Lafayette, IN

Quanghee Yi
Purdue University, West Lafayette, IN

Philippe L. Bourdeau
Purdue University, West Lafayette, IN

Follow this and additional works at: https://scholarsmine.mst.edu/icrageesd

Part of the Geotechnical Engineering Commons

Recommended Citation

ANALYTICAL STUDY OF THE NIKAWA LANDSLIDE

Dimitrios Loukidis
Purdue University
West Lafayette, IN 47907, USA

Sang-Ho Lee
Purdue University
West Lafayette, IN 47907, USA

Quanghee Yi
Purdue University
West Lafayette, IN 47907, USA

Philippe L. Bourdeau
Purdue University
West Lafayette, IN 47907, USA

ABSTRACT

One of the most severe landslides triggered by the 1995 Hyogoken-Nambu earthquake was the Nikawa landslide. The seismic ground motion generated excessive pore pressure inside the portion of the slope mass that was below the water table. Data from standard penetration tests suggested that, in spite of the significant percentage of fines in the sand and its slight overconsolidation due to the fluctuation of the water table, the slope material had potential of liquefaction under seismic loading. The objective of the present study was to investigate the consistency between observations and the results of analysis methods for this slope failure. The methods of analysis were the conventional method of slices for static and pseudo-static computations, the Newmark method, and numerical modeling using the finite differences program FLAC. The constitutive behavior of the sand in FLAC analyses was represented by a modified Mohr-Coulomb model incorporating the equation proposed by Martin , Finn and Seed (1975) for the volumetric strain increments due to cyclic loading. Using this formulation, it is possible to simulate the pore pressure build-up due to dynamic loading in the portion of the sand layer located below the water table. Results are discussed and compared with observations.

INTRODUCTION

In 1995, the Nikawa landslide took place in the residential area of the Nishinomiya city, a few kilometers from the center of Kobe. Under the seismic loading imposed by the Hyogoken-Nambu earthquake, the sliding mass moved more than 150m at high velocity. The failure occurred in an old man-made slope formed by a fill of non-compacted blue granitic sandy soil originating from the Osaka group geologic formation. The site conditions as described by Sassa et al. (1995), are shown in Fig.6. The Osaka group layer underlying the sandy fill is composed of sand and clay sublayers resting on a granitic base. The slight overconsolidation of the slope material was only due to fluctuations of the water table. Standard penetration tests performed after the event show N_{SPT} values for the undisturbed lower portion of the sand layer ranging from 4 to 16 with an average value close to 10 (Sassa et al, 1996).

Although the period, when the 1995 earthquake occurred, was dry, the relatively low permeability of the Osaka group formation kept the water table to a certain level (6-8m from ground surface). This resulted in the lower portion of the secondary sand deposit to be submerged, making this area prone to liquefaction upon seismic loading.

Sassa et al. (1996) performed cyclic consolidated-undrained ring shear tests using samples from the failed slope material. Prior to shearing, the samples were set to overconsolidation ratios 1.0 and 1.9. In both cases, pore pressure build-up continued after failure resulting in a fast drop of the effective stress path. The

shear resistance mobilized during motion corresponds to an apparent friction angle of $\phi_a=8.5°$. Although the stress paths generated during these tests could suggest flow liquefaction mechanism, there are some differences in the case of the slightly overconsolidated sample (OCR=1.9). According to Sassa et al. (1996) the pore pressure build-up that took place after the stress path reached the failure line was due to local liquefaction inside the narrow shear zone, where sand particles were crushed. Grain crushing was gradually generated after shear displacement of 1m. The ring shear tests provide useful information on the behavior of the slightly overconsolidated zones of the secondary sand deposit. However, given that the site is located in a region where the peak ground acceleration ranged between 0.5g and 0.85g and that the sand was not compacted, liquefaction may have taken place in an area broader than the local shear zone, first initiating and then accelerating the failure.

In the present paper, the slope failure is investigated using analytical and numerical approaches.

PSEUDOSTATIC APPROACH

On the basis of data published by Fukuoka et al. (1997), the distance of the Nikawa site to the fault rupture is approximately 1.5km. For this distance and earthquake magnitude M=7.2, the attenuation relationship proposed by Fukushima and Tanaka (1990) yields to a peak horizontal ground acceleration (PHGA) of 0.60g. Four ground accelerations records at distances between 0.8km and 3km from the fault line, on ground conditions similar

to the Nikawa site show peak values between 0.5g and 0.83g with a mean value of 0.66g (Ejiri et al., 1996). Considering that the center of the sliding mass was 7m below the ground surface, a PHGA of 0.6g is assumed herein for the pseudostatic stability analysis.
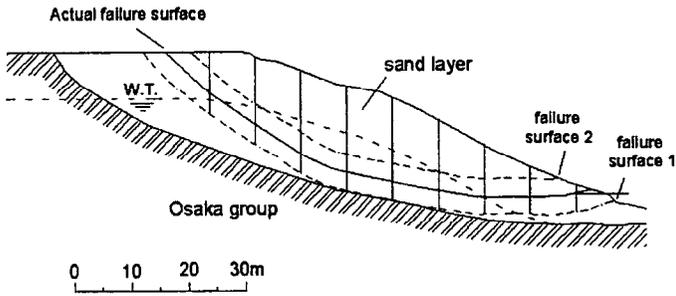

Fig. 1. Cross-section used for stability analysis showing the three considered failure surfaces and slices.

Three potential failure surfaces are considered (Fig.1), the actual failure surface and two surfaces obtained by its translation, 3m downwards (surface 1) and 3m upwards (surface 2). All three surfaces are located inside the sand layer. However, a portion of the lower surface coincides with the sand layer-Osaka group interface. The dry and wet unit weights of the sand are $17KN/m^3$ and $19KN/m^3$, respectively.

The potential sliding surfaces being approximately circular, the ordinary method of slices is applied with the discretization shown in Fig. 1. The safety factor is computed as

$$F.S. = \frac{\Sigma\{\tan\phi_{a_i} \cdot [(W_i \cdot \cos\beta_i - u \cdot D/\cos\beta_i) - W_i \cdot (a_h/g) \cdot \sin\beta_i]\}}{\Sigma\{W_i \cdot \sin\beta_i - W_i \cdot (a_h/g) \cdot \cos\beta_i\}} \quad (1)$$

where W_i is the weight, β_i is the inclination of the failure surface, $\phi_{a,i}$ the apparent friction angle for the slice (i), and a_h/g the seismic coefficient. Following suggestions by Hynes and Franklin (1984), a value of a_h=0.5·PHGA is adopted. The effect of the excess pore pressure Δu is introduced in the analysis through the apparent friction angle. Effective and apparent friction angles are related by

$$\tan\phi_a = \tan\phi' \cdot \left[1 - \frac{\Delta u \cdot D/\cos\beta}{W(\cos\beta - k \cdot \sin\beta) - u \cdot D/\cos\beta}\right] \quad (2)$$

where u is the initial pore pressure, Δu the earthquake induced excess pore pressure, D the width of slice and $k=a_h/g$. For slices entirely above the water table the effective friction angle ϕ'_{max} was used instead of the apparent angle. Using the Hatanaka and Uchida (1996) correlation between internal friction angle and SPT blowcounts number N_{SPT}

$$\phi'_{max}(°) = \sqrt{20 \cdot (N_1)_{60}} + 20 \quad (3)$$

, for an average value of N_{SPT} corrected with respect to the overburden pressure, equal to 10, ϕ_{max}=34°.

Results are presented in Fig. 2 for cases with and without earthquake and for values of ϕ_a ranging from 7° to 34°.
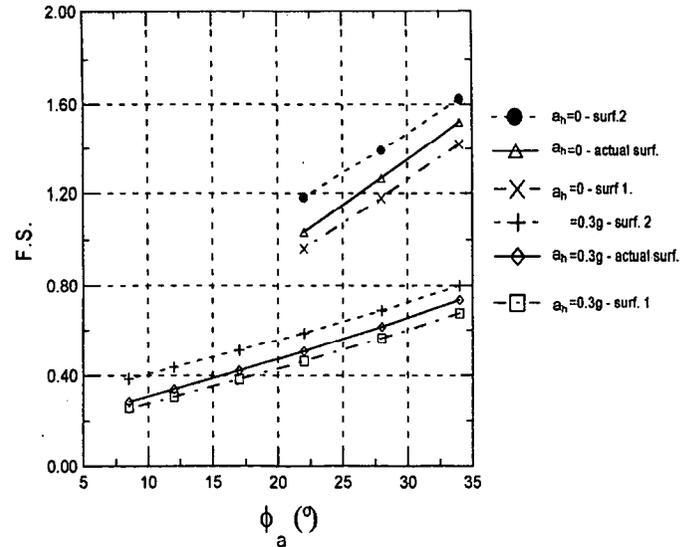

Fig. 2. Safety factors for the case without earthquake and for the case with earthquake a_h=0.3g (PHGA=0.6g) for the three assumed sliding planes.

It is observed that, within the range of friction angle considered, surface No. 1 gives safety factors slightly lower than those obtained for the actual failure surface. However, for values of the apparent friction angle near the experimental mobilized angle ϕ_a=8.5°, both surfaces yield practically the same value, F.S.=0.3. In every case where the seismic acceleration and the excess pore pressure are accounted for, the safety factor is clearly below 1.

Computations for static conditions and using the effective friction angle ϕ'_{max} result in a safety factor F.S.=1.42 with groundwater and F.S.=1.75 with a completely dry slope. The pseudo-static analysis indicates also that, for the PHGA conditions herein equal to 0.6g, even without development excess pore pressure (i.e. $\phi_a = \phi'_{max} = 34°$) the safety factor is less than 1 (i.e. F.S.=0.7). The peak ground acceleration that would cause initiation of sliding (min F.S.=1) with no effects of pore pressure build-up is PHGA=0.25g.

SLIDING BLOCK ANALYSIS

Using sliding block analysis method (Newmark, 1965), it was possible to assess the apparent friction angle mobilized on the failure surface required to produce fast sliding and long displacement under the effect of the earthquake.

Two accelerograms were used, recorded at JR Takarazuka station and JMA Kobe station, 1.2km and 0.6km from the rupture, respectively. Both accelerograms were scaled down to a peak acceleration of 0.6g. The yield acceleration was determined by the expression

$$a_y = g \cdot \tan(\phi - \beta) \quad (4)$$

where β is the average inclination of the observed sliding surface equal to 19.7°. For the integration of the accelerogram during the

Paper No. 5.31

2

first 1.5sec of excitation, the friction angle φ was set 34°. Then, between 1.5sec and 4.5sec, φ was reduced linearly to the value of the considered apparent friction angle φₐ. This is to account for the fact that the excess pore pressure did not develop immediately at the beginning of the earthquake. The time range between 1.5sec and 4.5sec was selected based on the numerical model presented in the next section. Examples of the scaled accelerogram and the corresponding sliding block analysis results are shown in Fig. 3.
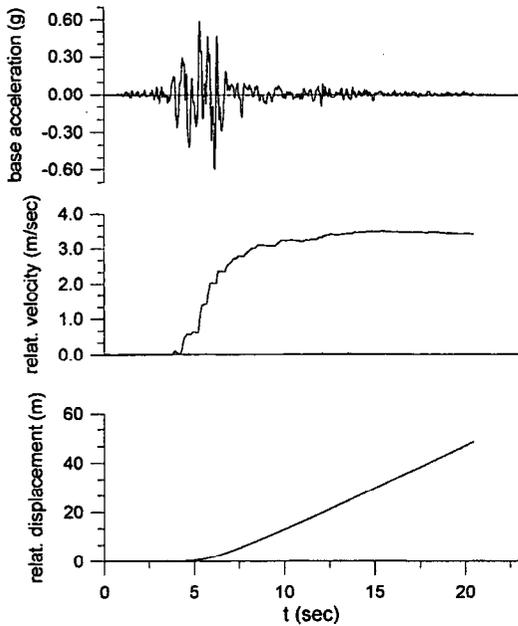

Fig. 3. Ground acceleration based on the JR Takarazuka record, , relative velocity and relative displacement after 20.5sec computed from rigid block analysis with φₐ=20°.
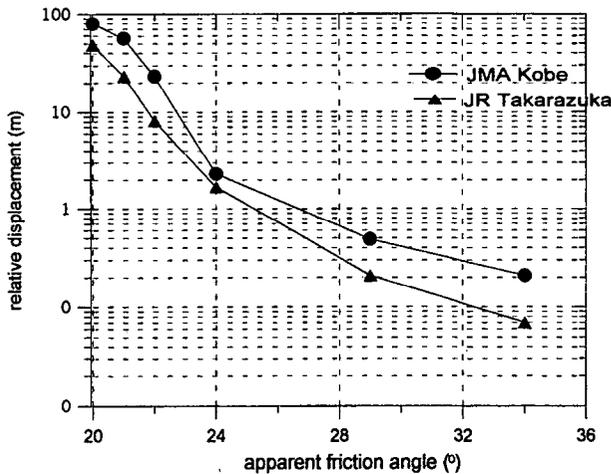

Fig. 4. Relative displacement after 20.5sec as a function of the assumed apparent friction angle mobilized during sliding.

Results of computations carried out for φₐ ranging between 34° and 20° are shown in Fig. 4. According to these results, for the large displacements observed at the Nikawa slide well beyond

80m to occur, the mobilized apparent friction angle had to be very small, typically lesser than 20°.

NUMERICAL SIMULATION

Model formulation

The FLAC finite differences program (Itasca Consulting Group, 1995) was used to perform fully coupled large strain analyses of the Nikawa landslide. Figure 5 shows the discretization grid used to model the soil profile. Initially, geostatic stresses are simulated in the model under elastic conditions. Then, an elastoplastic constitutive model with Mohr-Coulomb failure criterion and strain softening is set for the Osaka group, terrace deposits and the sand layer. The elastic model is kept throughout the analysis for the granite bedrock. The material constitutive parameters are summarized in Fig. 6.
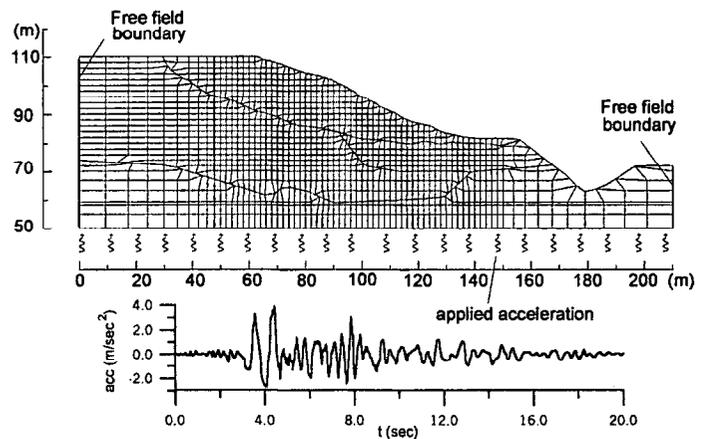

Fig. 5. Mesh (70x25) used in the finite difference analyses, and applied boundary conditions.

The peak friction angle for both the Osaka group and terrace deposits were assumed to be 48° and the cohesion 20KPa, since SPT data show N values up to 60. For the sand, friction angle was set equal to 34°. Based on relationships between shear wave velocity and N_{SPT} by Ohta and Goto (1978), it was considered that the shear modulus for the Osaka group and terrace was varying according to

$$G_{max} = 21062.5 \cdot \sigma_v'^{0.4} \quad (KPa) \qquad (5)$$

while for the sand layer

$$G_{max} = 9206.3 \cdot \sigma_v'^{0.4} \quad (KPa) \qquad (6)$$

where σ'ᵥ the effective vertical stress. The Poisson's ratio was set ν=0.25 for Osaka group-terrace deposits and 0.32 for the sand.

At first, it is verified that the system with the selected strength parameters is in equilibrium in absence of earthquake and with initial pore pressure. Instability to the model occurs by setting the friction angle of the sand φ=20°. To simulate excess pore pressure generation due to cyclic loading, the initially selected constitutive model for the embankment sand model is replaced
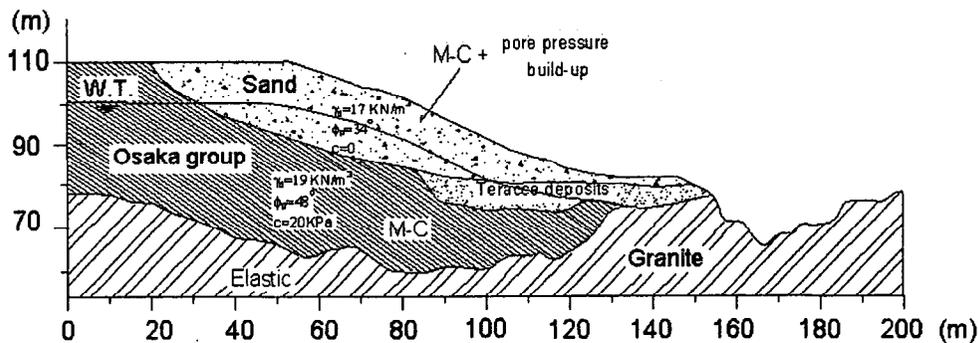
Fig. 6 Geological profile adapted by Sassa et al. (1996)and constitutive models selected for the numerical model. (M-C: elstoplastic model with Mohr-Coulomb failure criterion)

by a version of the Mohr-Coulomb elastoplastic model incorporating the equation (7) by Martin, Finn and Seed (1975). Equation (7) provides the volumetric strain increment $\Delta\varepsilon_{vd}$ due to cyclic loading

$$\Delta\varepsilon_{vd} = C_1 \cdot (\gamma_{cyc} - C_2 \cdot \varepsilon_{vd}) + \frac{C_3 \cdot \varepsilon^2_{vd}}{\gamma_{cyc} + C_4 \cdot \varepsilon_{vd}} \qquad (7)$$

where γ_{cyc} is the amplitude of each shear strain cycle and ε_{vd} the total accumulated volumetric strain. C_1, C_2, C_3 and C_4 are coefficients depending on the sand type and relative density. Using the coupled effective stress analysis in FLAC, excess pore pressure can be produced without introduction of expression involving the rebound modulus.

According to field observation the soil below the failure plane was blue granitic sand with a small percentage of silt and clay, originated from the Osaka group. Grain size distribution analyses performed by Sassa et al. (2000) show percentage of fines in the slope material about 20%. Based on representative strength liquefaction curves correlated with parameters C_1-C_4 by Martin et al. (1981), the values of theses constants are selected to be C_1=0.6, C_2=2.24, C_3=4.67 and C_4=4.79. These values correspond to a liquefaction strength curve that is also consistent with the cyclic stress ratio required to initiate liquefaction for sand with 20% fines and N_{SPT}=10 values, according to Seed et al. (1975).
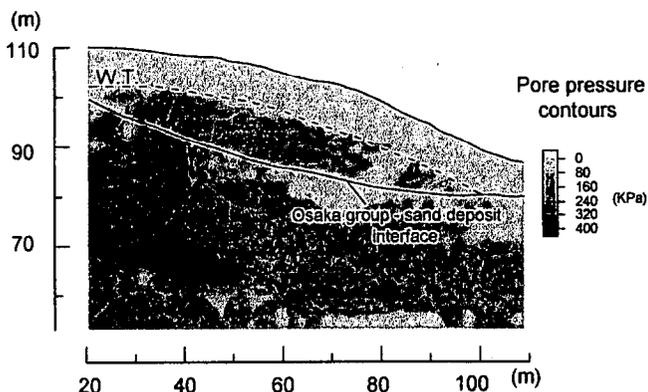

Fig. 7. Pore pressure contours after 8sec showing the excess pore pressure developed inside the submerged portion of the sand deposit.

Input ground motion

The earthquake acceleration is applied at the nodes of the bottom boundary. Since the motion is applied through the granite bedrock and the direction of the landslide was N60°E (Sassa, 2000), the most appropriate input motion is the one recorded at JMA Kobe station on stiff soil in the E-W direction. The average PHGA of three accelerograms recorded on rock at distances between 0.3km and 1.5km is 0.39g and the input acceleration was scaled at that target value. Free field conditions are introduced at the two lateral boundaries of the model.
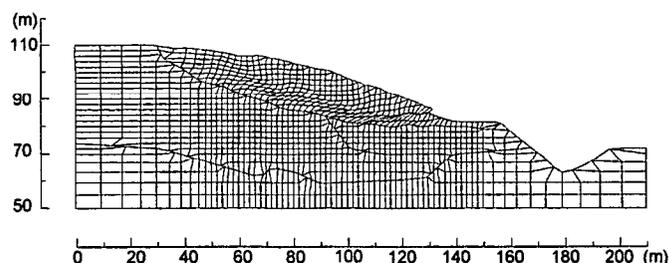
Results

Fig. 8. Deformed mesh after 8sec of simulated motion

The analysis with the constitutive model incorporating equation (7) shows a progressive pore pressure build-up inside a zone in the sand embankment, below the water table (Fig 7.). In consequence, a large portion of the embankment starts to slide along a shear band having maximum depth of 14 to 15m (Fig. 8). This shear band can be visualized from the shear strain increment contours (Fig. 9). The formed shear band is geometrically in agreement with the observed failure surface. The maximum horizontal displacement after 8.5 seconds of earthquake motion is about 8m.

The analysis could not proceed beyond the 8.5sec due to the extreme distortion of the elements lying on the shear band. However the computed horizontal velocities in the sliding mass up to 8.5sec of motion reach values of 0.6 to 1.2m/sec (Fig. 10). Such velocities seem high enough to lead us to the conclusion that the final displacement would be very large, as was actually observed.
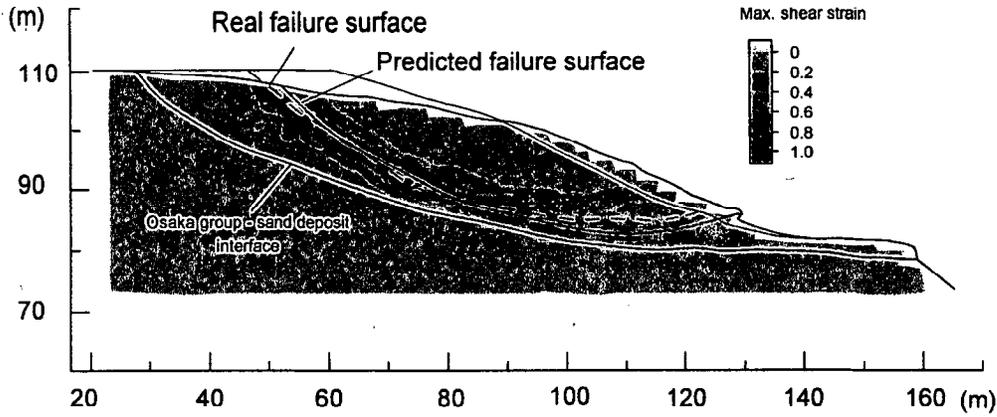
Paper No. 5.31

4

Figure 9: Shear strain contours after 8.5sec and displacement of the sliding mass 7.9m. Comparison between actual failure surface and shear zone developed in the numerical model.

During the analysis, pore pressure build-up reduced the mean effective stress to almost zero after 4.5 sec of motion (Fig. 11a). In Figure 11b, the effective stress path is shown in a p'-q diagram for an element in the shear zone. The stress path starts from an effective mean stress p'$_o$=180KPa and begins to

Fig.10. Horizontal velocity contour after 8.5sec of simulated motion..

increase progressively due to the increase of pore pressure. After several stress cycles the effective stress path reaches the failure line, corresponding to an effective friction angle of 34° and quickly drops downwards along the failure line due to continuous and fast increase of pore pressure. As the analysis proceeds, the stress path tend to oscillate around a point on the failure line, with q =22KPa. Thus, the predicted apparent friction angle is estimated to be

$$\phi_a = \sin^{-1}\left(\frac{q_f}{p'_o}\right) = \tan^{-1}\left(\frac{22}{180}\right) = 7° \qquad (9)$$

which is close to the experimental value of ϕ_a= 8.5° measured in the cyclic ring shear tests by Sassa et al. (1996).

In addition to the above simulation where pore pressure is allowed to develop freely in the model, the analysis was performed this time with a simpler constitutive model for the sand , which is the Mohr-Coulomb's with strain softening and
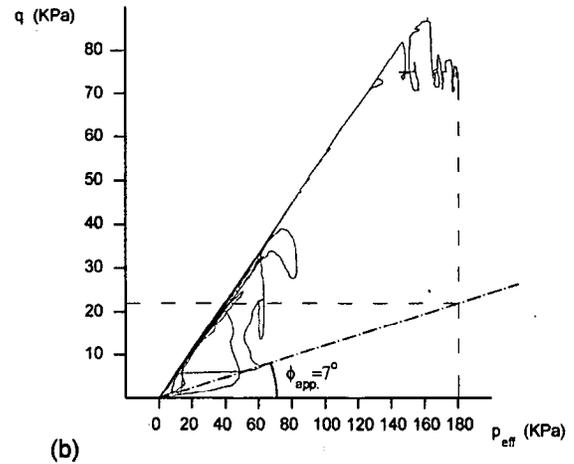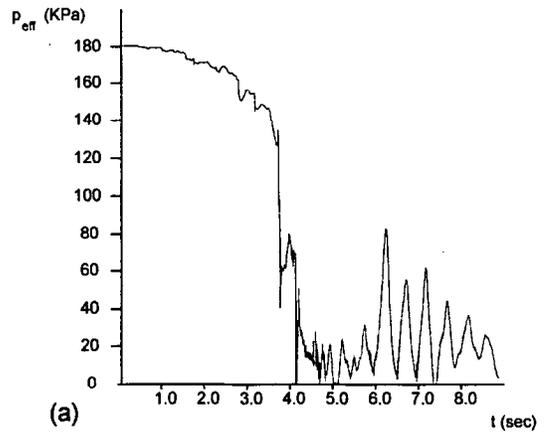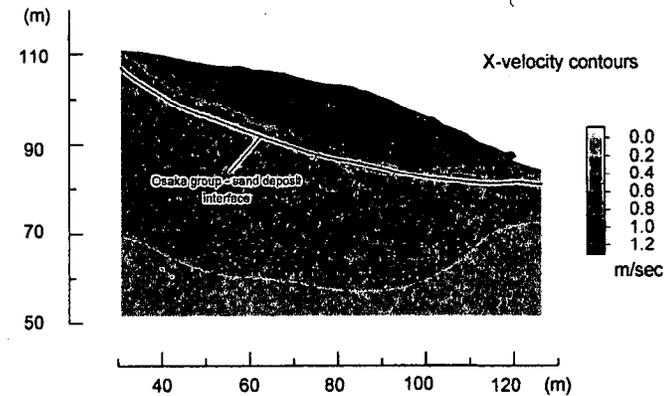

(a)

(b)

Fig.11. (a) Time history of the effective mean stress at element (27,16) located in the shear band. (b) Effective stress path for element (27,16).

water table below the sand layer. Using this formulation, development of excess pore pressure cannot affect the stability of the slope. Figure 12 shows that in this case, the model predicts only a superficial movement instead of a propagation of the failure zone deep inside the embankment mass, as observed in the first analysis.
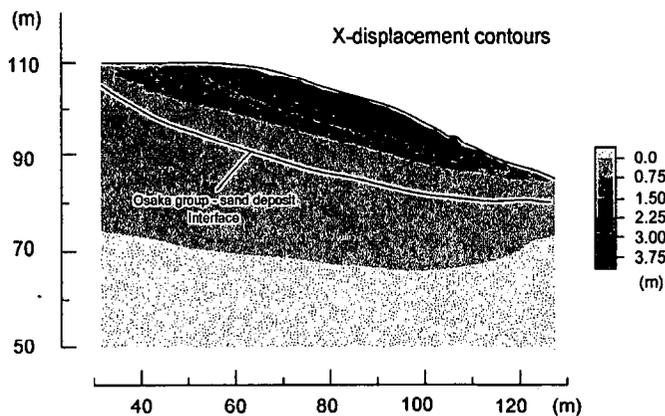
X-displacement contours

	0.0
	0.75
	1.50
	2.25
	3.00
	3.75
	(m)

Osaka group - sand deposit Interface

Fig. 12. Horizontal displacement contours after 15sec of motion in the analysis with water table below the sand layer deposit.

CONCLUSION

The failure zone formed in the numerical model during the dynamic analysis with possibility to predict pore pressure build-up is consistent with the observed failure surface. The numerical model indicated that, as consequence of the ground motion, large excess pore pressure developed in the portion of the embankment sand that was below the water table. The corresponding mobilized apparent friction angle, $\phi_a=7°$, was consistent with experimental data by Sassa et al. (1996) from undrained cyclic ring shear tests. The pseudo-static analysis and the sliding block method both indicate that with apparent friction angles as low as those anticipated, the ground shaking leads to slope failure and large displacements. Pseudo-static approach and numerical model show that the slope would be unstable under the experienced ground motion, even in absence of excess pores pressure. However the volume and displacement of the sliding mass in that case is significantly smaller.

ACKNOWLEDGEMENTS

REFERENCES

Disaster Prevention Research Institute [2000]. Landslide Section, Geo-Disasters Division, Disaster Prevention Research Institute, Kyoto University, http://landslide.dpri.kyoto-u.ac.jp .

Ejiri, J. , S. Sawada, Y. Goto, K. Toki [1996]. "Peak Ground Characteristics". Special Issue of Soils and Foundations, Japanese Geotechnical Society, pp. 7-13.

Fukuoka, H. , K. Sassa, G. S. Scararcia-Mugnozza [1997]. "Distribution of Landslides Triggered by the 1995 Hyogo-ken Nambu Earthquake and the Long run out Mechanism of the Takarazuka Golf Course Landslide". Journal of the Physics of Earth, Vol. 45, pp. 83-90.

Fukushima, Y., T. Tanaka [1990]. "A New Attenuation Relation for Peak Horizontal Acceleration of Strong Earthquake Ground Motion in Japan". Bulletin of the Seismological Society of America, Vol. 8, No.4, pp. 757-783.

Hatanaka, M., A. Uchida [1996]. "A simple method of determination of K_o value in sandy soils". Soils and Foundations, Japanese Geotechnical Society, Vol. 36, No.2, pages 94-99.

Hynes, M. E. and A. G. Franklin [1984]. "Rationalizing the Seismic Coefficient Method". Misc. Paper GL-84-13, U.S. Army Waterways Experiment Station, Vicksburg, MS.

Itasca Consulting Group [1995]. "FLAC: Fast Lagrangian Analysis of Continua, Version 3.3". User's Manual.

Martin, G.,W. Finn, H.B. Seed, [1975]. "Fundamentals of Liquefaction under Cyclic Loading". Journal of Geotechnical Engineering Division, ASCE, Vol . 101 (GT5), pp. 423-438.

Martin, G. R., I. P. Lam, S. L. McCaskie, C-F Tsai [1981]. "A Parametric Study of an Effective Stress Liquefaction Model". Proceedings, International Conference on Geotechnical Earthquake Engineering and Soil Dynamics. Vol. 2, St. Louis, MI, pp.699-705.

Newmark, N. M. [1965]. "Effect of Earthquakes on Dams and Embankments". Geotechnique, Vol. 15, No.2, pp. 139-160.

Ohta, Y. and N. Goto. [1978]. "Empirical Shear Wave Velocity Equations in Terms of Characteristic Soil Indexes". Earthquake Engineering and Structural Dynamics, Vol. 6, pp.167-187.

Sassa K., H. Fukuoka, T. Sakamoto [1995]. "The Rapid and Disastrous Nikawa Landslide". Landslide News, Japan Landslide Society, No. 9, pp. 6-9.

Sassa, K., H. Fukuoka, G.S. Muhnozza, S. Evans [1996]. "Earthquake-Induced-Landslides: Distribution, Motion and Mechanisms". Special issue of Soils and Foundations, pp. 53-64

Seed, H. B., K. Tokimatsu, L.F. Harder, R.M. Chung [1985]. "Influence of SPT procedures in soil liquefaction resistance evaluations". Journal of Geotechnical Engineering, ASCE, Vol. 111, No. 12, pp. 1425-1445.

Wang, F-W, K. Sassa and H. Fukuoka [2000]. "Geotechnical Simulation Test for the Nikawa Landslide Induced by January 17, 1995 Hoyogoken-Nambu earthquake". Soils and Foundations, Vol.40, No.1, pp. 35-46.